

ORIGINAL ARTICLE

Synergistic effect of ibrutinib and CD19 CAR-T cells on Raji cells in vivo and in vitro

Meijing Liu¹ | Xuelin Wang² | Zheng Li¹ | Rui Zhang³ | Juan Mu³  | Yanyu Jiang³ | Qi Deng³  | Lei Sun²

¹The First Central Clinical College of Tianjin Medical University, Tianjin, China

²Institute of Developmental Biology and Molecular Medicine, Fudan University, Shanghai, China

³Department of Hematology, Tianjin First Central Hospital, Tianjin, China

Correspondence

Qi Deng, Department of Hematology, Tianjin First Central Hospital, No. 24, Fukang Road, Nankai District, Tianjin, China.
Email: kachydeng@126.com

Lei Sun, Institute of Developmental Biology and Molecular Medicine, Fudan University, Room 5002, Yifu technology building, 220 Handan road, Shanghai, China.
Email: lei_sun@fudan.edu.cn

Abstract

Ibrutinib might improve the efficacy of anti-CD19 chimeric antigen receptor (CD19 CAR) T-cell therapy in chronic lymphocytic leukemia (CLL). We studied the possibility and mechanism of the synergistic effect of ibrutinib and CAR-T cells in other types of lymphoma. In this study, we selected the CD19 CAR-T cells of a patient with lymphoma who failed in his CD19 CAR-T-cell therapy and a dose of 8 mg/kg/d ibrutinib. Subcutaneous and tail vein tumorigenic mice were established with Raji cells. The differences in the synergistic effect between these 2 models were compared by bioluminescence imaging (BLI) monitoring and flow cytometry (FCM). The expression of the STAT-3 signaling pathway was assessed by western blot analysis. There was no synergistic effect of ibrutinib and CD19 CAR-T cells in vitro. Programmed cell death-ligand 1 (PD-L1) was expressed in $0.23 \pm 0.06\%$ of Raji cells. In the subcutaneous tumorigenic model, the luciferase signal was reduced significantly in the group receiving ibrutinib combined with CD19 CAR-T cells. Moreover, the proportion of CD19 CAR-T cells was higher in the polytherapy group than in the CAR-T-cell monotherapy group. However, we did not get an analogous synergistic effect in the tail vein tumorigenic model. STAT-3 signaling pathway expression in the residual tumor cells did not differ between those with and those without ibrutinib, suggesting that the IL-10/STAT-3/PD-L1 pathway was not involved in the synergistic effect. Therefore, some other mechanism might be a target for ibrutinib. Our results provide evidence for the use of ibrutinib in polytherapy for other types of B-cell lymphoma.

KEYWORDS

Bruton tyrosine kinase inhibitor, chimeric antigen receptor, programmed cell death-ligand 1, Raji cell line, tumor microenvironment

Qi Deng and Lei Sun contributed equally to this work.

Trial registration: The patients were enrolled in a clinical trial ChiCTR1800018059.

This is an open access article under the terms of the Creative Commons Attribution-NonCommercial-NoDerivs License, which permits use and distribution in any medium, provided the original work is properly cited, the use is non-commercial and no modifications or adaptations are made.

© 2020 The Authors. *Cancer Science* published by John Wiley & Sons Australia, Ltd on behalf of Japanese Cancer Association

1 | INTRODUCTION

As a Bruton tyrosine kinase (BTK) inhibitor, ibrutinib controls homing and migration of tumor cells by downregulating NF- κ B signaling. It is important to block the interactions between macrophages and tumor cells.¹⁻⁴ Abnormal B-cell receptor (BCR) signaling is a key mechanism of B-cell malignancy disease progression. BTK has a pivotal role in BCR signaling.^{5,6} By blocking BTK, ibrutinib inhibits BCR signaling in cells of B-cell malignancies^{7,8} and has been approved by the FDA for the treatment of chronic lymphocytic leukemia (CLL)⁹ and mantle cell lymphoma (MCL)¹⁰ in all lines of therapy. Moreover, ibrutinib has been used widely in different types of B-cell malignancies of the lymphatic system.¹¹⁻¹³ Although the overall response rates (ORR) to ibrutinib in patients with CLL or MCL are high, the complete response (CR) rate is low, and some patients experience disease progression while receiving ibrutinib.^{14,15}

Anti-CD19 chimeric antigen receptor (CD19 CAR) T-cell therapy achieved high response rates in patients with relapsed/refractory (R/R) diffuse large B-cell lymphoma (DLBCL)^{16,17} and R/R B acute lymphoblastic leukemia (B-ALL).¹⁸ Additionally, CD19 CAR-T-cell therapy was also used in CLL,^{19,20} but the efficacy was lower for CLL than for DLBCL or B-ALL.¹⁶⁻¹⁸ A previous study evaluating the safety and feasibility of CD19 CAR-T-cell therapy in CLL patients who received ibrutinib suggested that ibrutinib might improve the efficacy of CD19 CAR-T-cell therapy.²¹ A similar synergistic effect was reported in MCL models.²² Specifically, the cytotoxicity of CD19 CAR-T cells to MCL cells was significantly enhanced with the assistance of ibrutinib. In our study, the Raji cell line was selected to study the effects of polytherapy with ibrutinib and CD19 CAR-T cells both in vitro and in vivo. The synergistic effect of ibrutinib combined with CD19 CAR-T cells was observed in the subcutaneous tumorigenic model, but not in the tail vein tumorigenic model. Taken together, our data suggested that ibrutinib might have a synergistic effect with CD19 CAR-T cells by improving the tumor microenvironment.

2 | MATERIALS AND METHODS

2.1 | Primary cells and cell lines

Nine patients with R/R DLBCL (men:women = 5:4, age: 31-63 y) were enrolled in a clinical trial at the Department of Hematology, Tianjin First Center Hospital (Tianjin, China). The patients received CD19 CAR-T cells expressing anti-CD19 scFv and 4-1BB-CD3 ζ costimulatory-activation domains (*ChiCTR1800018059*). All patients or their representatives provided informed consent before enrollment. They agreed to the use of their specimens and data for our study.

Raji and U-2932 cells (American Type Culture Collection, ATCC) were cultured in RPMI-1640 medium (Gibco; Thermo Fisher Scientific, Inc) containing 10% fetal bovine serum (FBS) (Gibco, Thermo Fisher Scientific, Inc) and 50 UI/mL penicillin/streptomycin (Gibco, Life Technologies). Human embryonic kidney 293 (Lenti-X-293T) cells (ATCC) were maintained in Dulbecco's modified Eagle's

medium (Sigma-Aldrich) supplemented with 10% FBS and 50 IU/mL penicillin/streptomycin.

2.2 | Isolation of peripheral blood mononuclear cells (PBMCs) and transduction of T cells

PBMCs from 9 patients were isolated by Ficoll density gradient centrifugation. CD3⁺ T cells were separated from the PBMCs by magnetic cell sorting (MACS) using CD3 microbeads (Miltenyi Biotec, Inc). CD3⁺ T cells were stimulated with anti-CD3/anti-CD28 mAb-coated Human T-Expander beads (cat. no. 11141D; Thermo Fisher Scientific, Inc) and cultured in T-cell medium X-Vivo 15 (Lonza Group, Ltd.) supplemented with 250 IU/mL interleukin-2 (IL-2; Proleukin; Novartis International AG). On the fourth day of culture, T cells (3×10^6) were transduced with a lentiviral vector encoding anti-CD19 CAR constructs (5 μ g; lenti-EF1a-CD19-2rd-CAR; Creative Biolabs, Inc) and cultured in medium containing recombinant human IL-2 (250 IU/mL). At the same time, CD3⁺ T cells were cultured in T-cell medium X-Vivo 15 supplemented with 250 IU/mL interleukin-2. On the 12th day of culture, the transduction efficiency of CAR 19 was analyzed by flow cytometry (FCM) to detect the ratio of CAR-T 19 cells in CD3⁺ T cells.

2.3 | Pharmacologic agents

The BTK inhibitor ibrutinib was provided by Xian Janssen Pharmaceutical Co. Ltd. Ibrutinib was dissolved in dimethyl sulfoxide (DMSO) to make a 10-mmol/L stock solution, and stored in small aliquots at -20°C .

2.4 | Proliferation of CD19 CAR-T cells and cell lines in vitro

The effects of different doses of ibrutinib on CD19 CAR-T cells or cell line proliferation were determined using a Cell Counting Kit-8 (CCK-8; Dojindo Molecular Technologies, Inc). CD19 CAR-T cells or cell lines were seeded into 96-well plates at 3×10^4 cells per well and treated with various doses of single-agent ibrutinib. Absorbance was measured at 450 nm at 24, 48, and 72 h using an enzyme standard instrument. All assays were run in duplicate or triplicate.

2.5 | Expression of programmed cell death protein 1 (PD-1) on CAR-T cells, programmed cell death-ligand 1 (PD-L1) on cell lines, and immune phenotype of T lymphocytes

In the preparation process for CD19 CAR-T cells, the expression of PD-1 was analyzed by FCM. When the CAR-T cells were harvested, the expression of PD-1 was analyzed by FCM in the co-culture system containing ibrutinib or Raji cells for 24 and 48 h.

The effector:target ratio was 1:1, and the ibrutinib concentration was 5 $\mu\text{mol/L}$. PD-L1 expression in Raji and U-2932 cells was analyzed by FCM.

The T-lymphocyte immune phenotype of 9 patients was detected after culturing T lymphocytes with 5 $\mu\text{mol/L}$ ibrutinib for 72 h *in vitro*. Analysis included naive T cells, effector T cells, central memory T cells, and effector memory T cells in $\text{CD3}^+\text{CD4}^-\text{CD8}^+$ T cells and $\text{CD3}^+\text{CD4}^+\text{CD8}^-$ T cells. We evaluated the percentage and absolute numbers of T cells of various subsets.

2.6 | Cytotoxicity assays

Cytotoxicity assay was carried out at an effector:target ratio of 1:1 for 24 and 48 h in the absence of supplemented cytokines. Ibrutinib concentration was at 0, 1, and 10 $\mu\text{mol/L}$ combined with CD19 CAR-T cells. As controls, targets (2×10^4 cells per well) and effectors (2×10^4 cells per well) alone were incubated simultaneously to determine spontaneous cell death. Cytotoxicity was detected using a lactate dehydrogenase (LDH) cytotoxicity test kit (Dojindo Molecular Technologies, Inc) at 490 nm. All assays were run in duplicate or triplicate.

2.7 | Xenograft tumor model

Here, 6-wk-old female CAnN.Cg-Foxn1nu/CrIVR (BALB/c) mice weighing 20.12 ± 1.45 g ($n = 50$; Beijing Vitonlihua Experimental Animal Technology Co., Ltd) received 1×10^7 Raji cells transduced with luciferase (purchased from Shanghai Super Biotechnology Co.) by subcutaneous injection, followed by bioluminescence imaging (BLI) monitoring twice a week. Upon confirmation of engraftment after 25 d, the mice were randomized into an ibrutinib (8 mg/kg/d) monotherapy group, a CD19 CAR-T-cell ($2 \times 10^7/\text{kg}$) monotherapy group, an ibrutinib combined with CD19 CAR-T cells group, and an ibrutinib combined with T cells ($2 \times 10^7/\text{kg}$) group. The CD19 CAR-T cells and T cells generated from the same donor (patient no. 7 who did not respond to CAR-T-cell therapy) were administered to the tail vein on day 0. Ibrutinib was administered daily to the mice by oral gavage. There were 5 mice in each group. On day 0, day 14, and day 28, mice were monitored using BLI for disease progression following intraperitoneal injection with D-luciferin (Goldbio, 150 mg/kg) 10 min before scanning. Before imaging, mice were anesthetized via a nose cone with 2% isoflurane (Zoetis) medical oxygen and maintained under inhalational anesthesia. All mice were sacrificed when either experimental or human endpoints were reached.

Another group of the same mice was injected with 1×10^7 Raji lymphoma cells by tail vein injection to establish an animal model. Upon confirmation of engraftment after 10 d, these mice were separated randomly into various groups as in the subcutaneous tumorigenic mouse models. The CD19 CAR-T cells, T cells, and ibrutinib were utilized in the same way as in the subcutaneous tumorigenic mouse models. There were 5 mice in each group. The

proportions of lymphoma cells in the epicanthus vein on days 0, 7, 14, 21, and 28 were analyzed by FCM. The proportions of lymphoma cells in the bone marrow on day 21 were also analyzed by FCM.

2.8 | Change of CD19 CAR-T cells ratio in mice

Inner canthus blood was collected from the mice of the CAR-T-cell group and ibrutinib combined with the CAR-T-cell group on days 0, 7, 14, 21, and 28. The proportions of CD19 CAR-T cells in mice were analyzed by FCM.

2.9 | Western blot analysis of phospho-signal transducer and activator of transcription 3 (STAT-3)

In the subcutaneous tumorigenic model, we chose the ibrutinib group and the polytherapy group (CD19 CAR-T cells and ibrutinib) in the following western blot analysis. The residual tumor tissue in subcutaneous nodules was taken and milled to obtain tumor cells following mice sacrifice after 28 d of therapy. Tumor cells were selected by CD19 magnetic beads for the following experiments. CD19^+ tumor cells (Raji cells) were plated at 0.5×10^6 per well (6-well plate) for 0, 24, and 72 h. The cells were collected and dissolved in 200 μL Laemmli buffer (Bio-Rad). Next 10 μL of each protein sample were loaded onto SDS-PAGE gels (Bio-Rad) and transferred to PVDF membranes. Antibodies against STAT-3 (Ser727), STAT-3, and GAPDH were applied and detected using the corresponding secondary antibodies. Total and phosphorylated proteins were detected using an enhanced chemiluminescence detection system.

2.10 | Statistical analysis

All statistical analyses were performed using GraphPad Prism 7 (GraphPad Software, Inc) and SPSS version 23 (IBM Corp.). Data were expressed as the mean \pm standard deviation (SD) or standard errors of the mean (SEM). Inter-group comparisons were performed using *t* test, one-way ANOVA, and two-way ANOVA where indicated. ANOVA (Student-Newman-L method) was used for pairwise comparisons. Differences were considered significant at values of $P < .05$.

3 | RESULTS

3.1 | Patients' characteristics and transduction efficiency of CD19 CAR-T cells

Five male and 4 female R/R DLBCL patients with a median age of 52 y (range: 31-63 y) were enrolled in our clinical trial. The molecular

TABLE 1 Characteristics of 9 patients with relapsed/refractory diffuse large B-cell lymphoma

Patient number	Age	Sex	Molecular subtype	Stage	Previous response status	International prognostic index at enrollment	Number of therapies received before
P1#	31	Female	Non-GCB	III	Refractory	3	12
P2#	56	Male	Non-GCB	IV	Relapse	3	8
P3#	35	Male	Non-GCB	III	Relapse	3	8
P4#	52	Male	Non-GCB	IV	Relapse	3	14
P5#	54	Female	Non-GCB	IV	Refractory	3	10
P6#	50	Male	Non-GCB	IV	Relapse	2	12
P7#	58	Male	Non-GCB	IV	Refractory	3	7
P8#	63	Female	Non-GCB	IV	Refractory	5	13
P9#	50	Female	Non-GCB	IV	Refractory	3	20

subtypes, the stages based on the modified Ann Arbor staging system, and the international prognostic index (IPI) scores are shown in Table 1. The titer of anti-CD19-CAR virus was 3×10^8 TU/mL. Mean anti-CD19-CAR transduction efficiency of the 9 R/R DLBCL patients was $58.62 \pm 6.18\%$. The anti-CD19-CAR transduction efficiency of patient no. 7 was 54.34%.

3.2 | Medical history and the CD19 CAR-T-cell therapy of patient no. 7

We selected CD19 CAR-T cells from patient No. 7 for experiments in vitro and in vivo. Patient no. 7 was a 58-y-old man who suffered from multiple cervical lymph nodes enlargement in September 2015. The patient was diagnosed by cervical lymph node biopsy as presenting with germinal center B-cell (GCB) DLBCL. He had a high-grade B-cell lymphoma with MYC rearrangement plus rearrangement of BCL-6 genes. After 6 cycles of R-CHOP combined chemotherapy, the patient achieved his first CR. The patient did not receive autologous hematopoietic stem cell transplantation and other maintenance treatments. The size of his cervical lymph nodes increased again in April 2017. He did not benefit from 2 cycles of dexamethasone, Ara-C, and cisplatin (DHAP) combined chemotherapy. The immunohistochemistry (IHC) results of lymph node tissue from patient no. 7 showed strong CD19 positivity (Figure 1A). Therefore, he was enrolled in this clinical trial for CD19 CAR-T-cell therapy. The viability of CD19 CAR-T cells from patient no. 7 was low. PD-1 expression on CD3⁺ T cells was higher in patient no. 7 than in other patients ($P < .0001$), and there was no difference in the transduction efficiency between the 9 patients (Figure 1B). The release of interferon-gamma (IFN- γ) in this patient was lower than in other patients, following co-culture of CAR-T cells and Raji cells or U-2932 cells at 48 h ($P < .0001$) (Figure 1C). However, there was no difference in the proliferation of CAR-T cells between patient no. 7 and other patients following cell culture (Figure 1D). PD-1 expression on T cells and CAR-T cells from patient no. 7 declined in culture (Figure 1E). The levels of CD19 CAR-T cells and cytokines during CD19 CAR-T cell therapy

for patient no. 7 were very low (Figure 1F,G). Unfortunately, his disease progressed during therapy (Figure 1H).

3.3 | Effect of different doses of single-agent ibrutinib on proliferation of CD19 CAR-T cells and different cell lines

The effect of ibrutinib on the proliferation of CAR-T cells was investigated first on the day 12 of culture to analyze the combined effects of ibrutinib and CAR-T cells. CD19 CAR-T cells were incubated with ibrutinib at doses of 0, 1, and 10 $\mu\text{mol/L}$. We determined the inhibitory effects of ibrutinib on CD19 CAR-T-cell growth, as reflected by cell density after 24 and 48 h (Figure 2A). Noticeably higher ibrutinib concentration was associated with decreased survival of CAR-T cells. Notably, 72 h treatment with 10 $\mu\text{mol/L}$ ibrutinib almost 'swept out' CAR-T-cell incubation, indicating the importance of proper ibrutinib dosage for polytherapy strategy.

We next analyzed the toxicity of ibrutinib on malignant B cells in vitro. Cell survival was measured in Raji cells and U-2932 cells treated with ibrutinib at 0, 1, or 10 $\mu\text{mol/L}$ doses for 24 and 48 h. Proliferation was inhibited at 48 h more strongly in the 10 $\mu\text{mol/L}$ ibrutinib group for U-2932 cells and Raji cells rather than in the 1 $\mu\text{mol/L}$ ibrutinib groups (Figure 2B,C).

3.4 | Cytotoxicity of CD19 CAR-T cells for Raji cells or U-2932 cells

CD19 CAR-T-cell monotherapy was conducted in vitro to test the cytotoxic capability of CAR-T cells from different patients. CD19 CAR-T cells were cultured with Raji cells or U-2932 cells to determine cytotoxicity using the LDH assay. We showed significant cytotoxicity of CD19 CAR-T-cells from all patients except no. 7 toward U-2932 cells or Raji cells (effector:target ratio 1:1) at 24 and 48 h. However, CD19 CAR-T cells from patient no. 7 showed limited cytotoxicity to Raji cells or U-2932 cells at 24 and 48 h (Figure 2D,E).

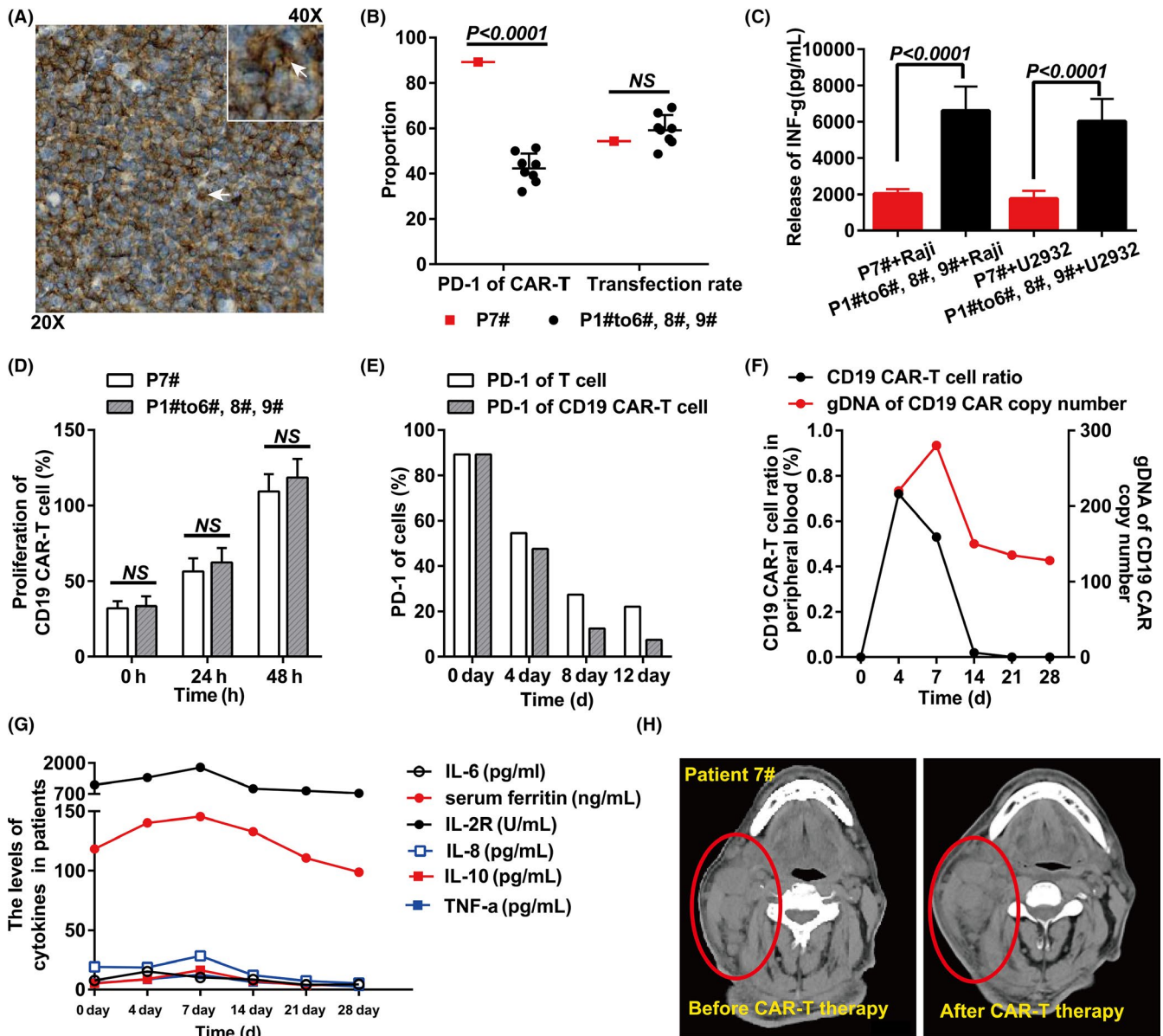


FIGURE 1 A, Immunohistochemistry of lymph node tissues from patient no. 7 showed strong CD19 expression (brown staining, white arrow points). B, Expression of programmed cell death protein 1 (PD-1) on CD3⁺ T cells from patient no. 7 was higher than in other patients ($P < .0001$). There was no difference in the transduction efficiency of the 9 patients. C, Release of interferon-gamma (IFN- γ) in patient no. 7 was lower than in other patients at 48 h ($P < .0001$). D, There was no difference in the proliferation of anti-CD19 chimeric antigen receptor (CAR)-T cells in culture between patient no. 7 and other patients. E, PD-1 expression on the T cells and CAR-T cells in culture declined in patient no. 7. F, G, CD19 CAR-T-cell and cytokines in the CD19 CAR-T-cell therapy. H, Evaluation of CD19 CAR-T-cell therapy effects by computerized tomography in patient no. 7

3.5 | Changes in PD-1 expression in CAR-T cells co-cultured with ibrutinib and Raji cells, and PD-L1 expression in cell lines

Harvested CD19 CAR-T cells were co-cultured with ibrutinib and Raji cells. PD-1 expression increased in CAR-T cells co-cultured with Raji cells after 48 h, whereas in CAR-T cells co-cultured with ibrutinib and Raji cells, PD-1 expression was lower than in CAR-T cells co-cultured with Raji cells only (Figure 2F). Results of 3 repetitions of the experiment showed that PD-L1 expression was $0.23 \pm 0.06\%$ in Raji cells and $40.55 \pm 3.18\%$ in U-2932 cells.

3.6 | Combined effect of ibrutinib and CD19 CAR-T cells

Cytotoxicity of CD19 CAR-T cells combined with ibrutinib at 0, 1, or 10 $\mu\text{mol/L}$ doses at 24 and 48 h after co-culture with Raji cells and U-2932 cells was analyzed. No combined effects of CD19 CAR-T cells with ibrutinib to Raji cells and U-2932 cells were found (effector:target ratio was 1:1) at 24 and 48 h in patient nos. 1-6, 8, and 9. CD19 CAR-T cells from patient no. 7 treated with ibrutinib showed almost no cytotoxicity to Raji and U-2932 cells at 24 and 48 h (Figure 3A,B).

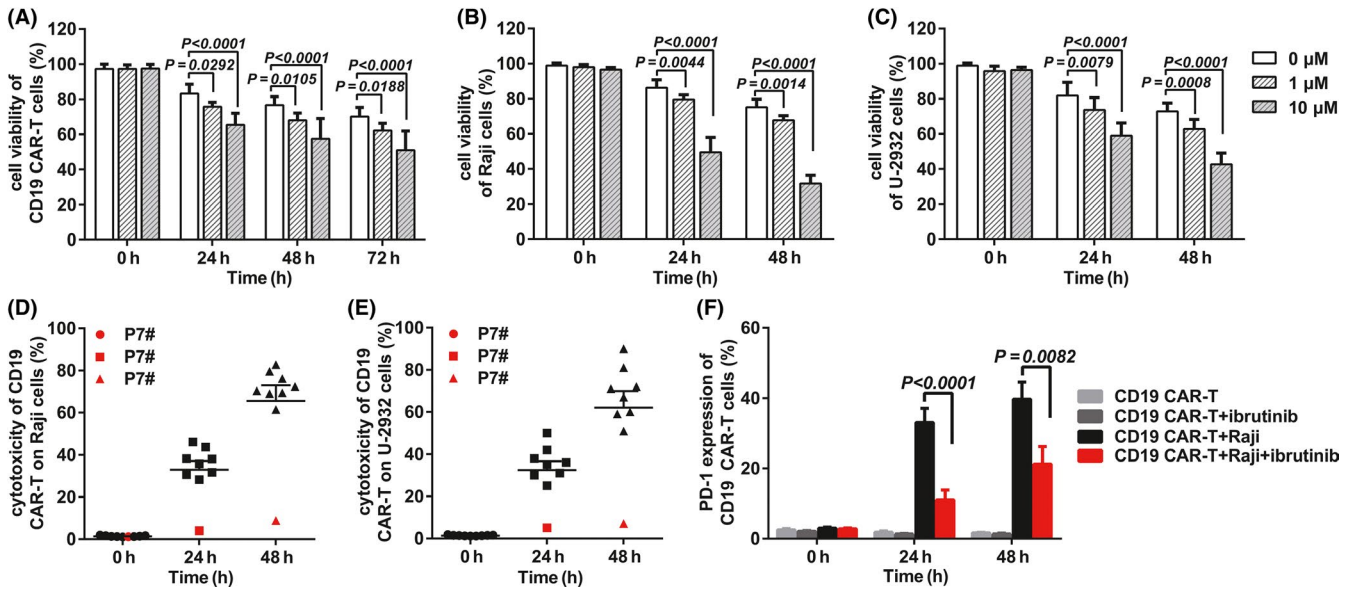


FIGURE 2 Effect of different doses of ibrutinib on cells. A, Effect of different doses of ibrutinib on anti-CD19 chimeric antigen receptor (CAR)-T cells. B, C, Effect of different doses of ibrutinib on Raji cells and U-2932 cells. D, Cytotoxicity of CD19 CAR-T cells from 9 patients on Raji cells. E, Cytotoxicity of CD19 CAR-T cells from 9 patients on U-2932 cells. F, Expression of programmed cell death protein 1 (PD-1) in CAR-T cells increased by co-culture with Raji cells and decreased by co-culture with ibrutinib and Raji cells. PD-1 expression in CAR-T cells co-cultured with ibrutinib and Raji cells was lower than in those cells co-cultured with Raji cells only

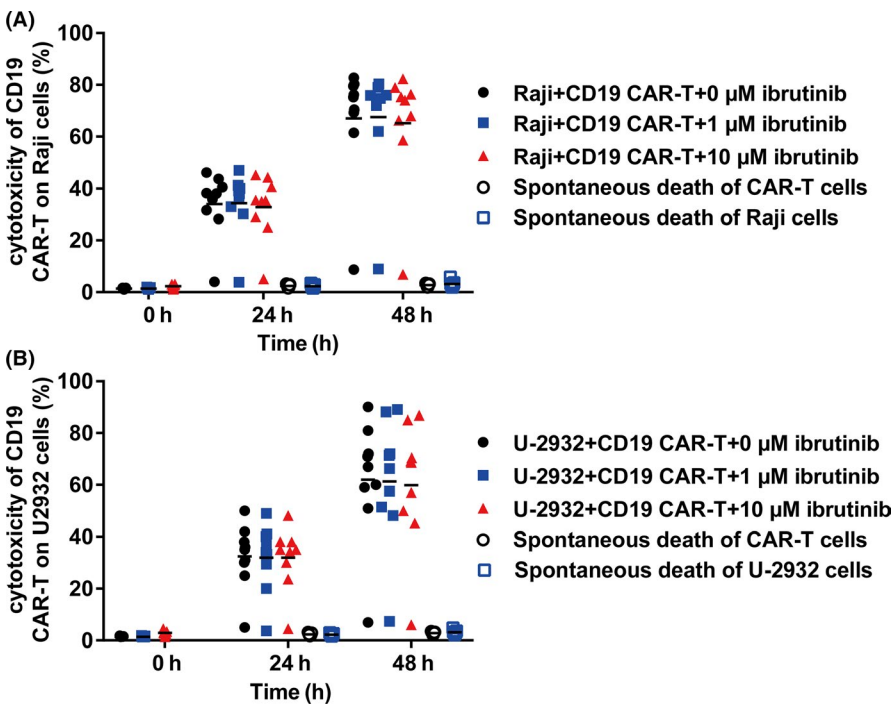


FIGURE 3 Combined effect of ibrutinib and anti-CD19 chimeric antigen receptor (CAR)-T cells in vitro. A, B, There were no combined effects of CD19 CAR-T cells with ibrutinib on Raji cells and U-2932 cells in vitro. The CD19 CAR-T cells of patient no. 7 showed almost no cytotoxicity to cell lines with or without ibrutinib

3.7 | Immune phenotype of T lymphocytes in all 9 patients

We evaluated the percent of various subsets and absolute numbers of T cells from 9 patients cultured with 5 $\mu\text{mol/L}$ of ibrutinib. There was no difference in the percentage and absolute numbers of the naive T cells, effector T cells, central memory T cells, and effector memory T cells in $\text{CD}3^+\text{CD}4^-\text{CD}8^+$ T cells and $\text{CD}3^+\text{CD}4^+\text{CD}8^+$ T cells (Figure 4).

3.8 | Antitumor efficacy of ibrutinib and CD19 CAR-T cells in the subcutaneous tumorigenic model

We performed the following mouse experiments with the CD19 CAR-T cells from patient no. 7, who had failed in CD19 CAR-T-cell therapy. In the subcutaneous tumorigenic model, neither of the 4 groups (the single-agent ibrutinib, CD19 CAR-T cells, ibrutinib combined with CD19 CAR-T cells, and ibrutinib combined with T cells

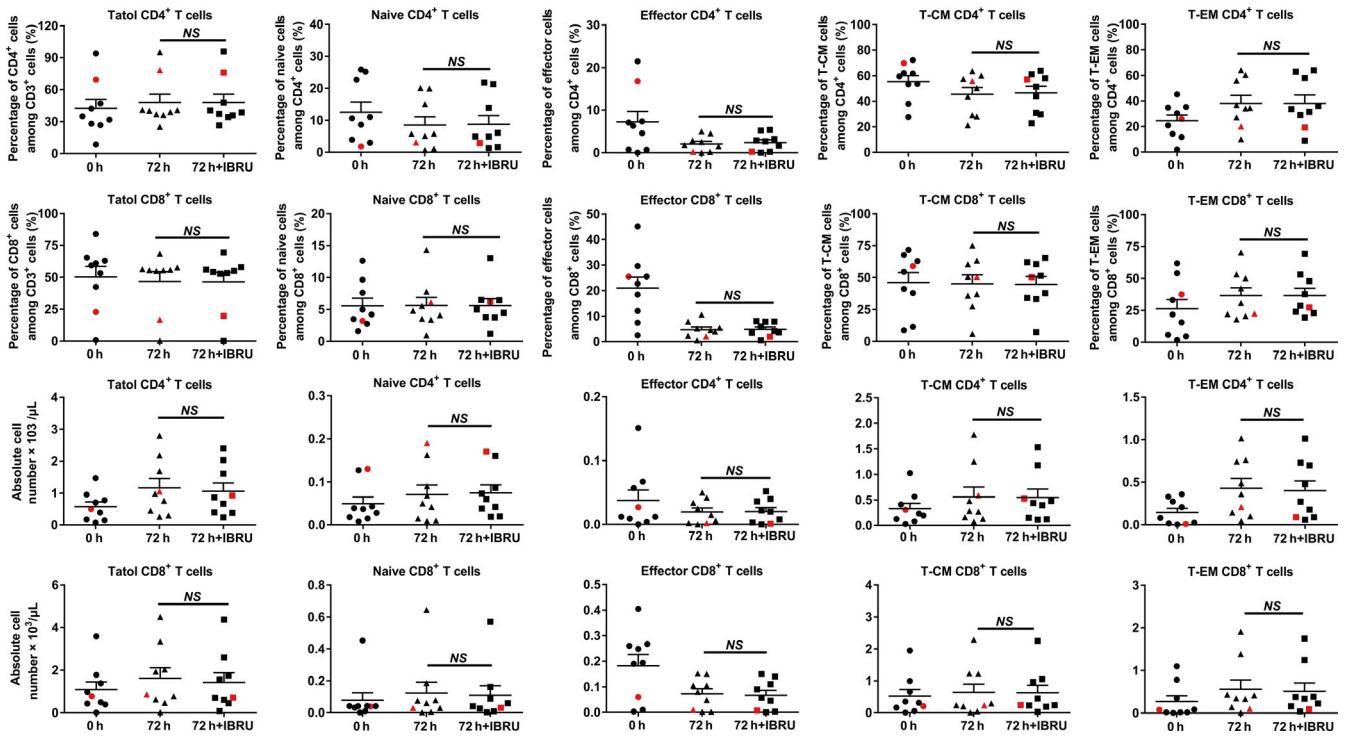


FIGURE 4 Immune phenotype of T lymphocytes in all 9 patients. There were no differences in the percentage and absolute numbers of naive T cells, effector T cells, central memory T cells, and effector memory T cells in CD3⁺CD4⁻CD8⁺ T cells and CD3⁺CD4⁺CD8⁻ T cells. Data of patient no. 7 in the figure are identified in red

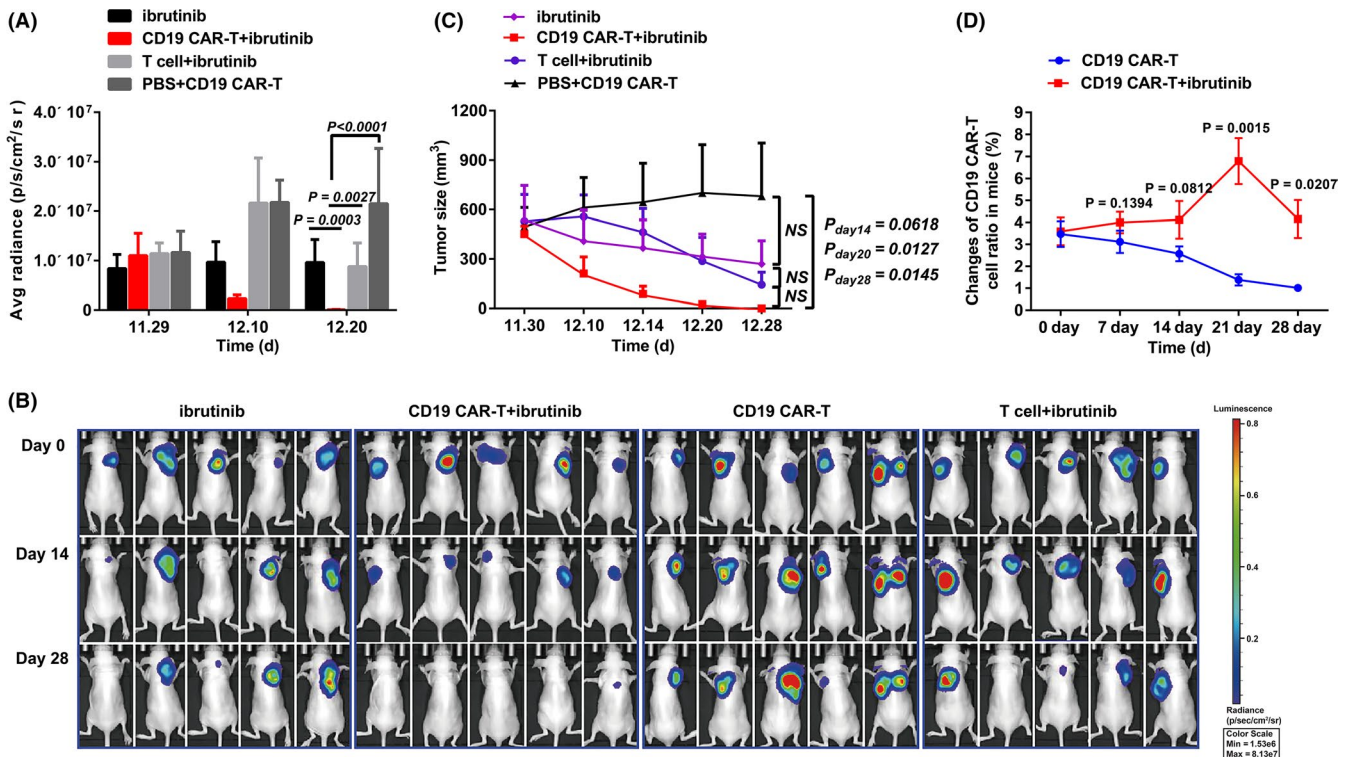


FIGURE 5 Combined effect of ibrutinib with CD19 CAR-T cells in the subcutaneous tumorigenic model. A, B, Decrease in luciferase expression was greater in the ibrutinib combined with CD19 CAR-T-cell polytherapy group than in the other 3 groups. C, Reduction in tumor size was greater in the ibrutinib combined with CD19 CAR-T-cell polytherapy group than the CAR-T-cell alone group. D, Proportion of CD19 CAR-T cells was higher in the ibrutinib combined with CD19 CAR-T-cell polytherapy group than in the CD19 CAR-T-cell group on day 21 and day 28

group) presented detectable toxicities, all of them maintained overall weight. The extinction of luciferase expression in the ibrutinib combined with CD19 CAR-T-cell group was greater than that in the ibrutinib group ($P_{\text{day}28} = 0.0003$), the ibrutinib combined with T-cell group ($P_{\text{day}28} = 0.0027$) and the CAR-T-cell alone group ($P_{\text{day}28} < 0.0001$) (Figure 5A,B). Treatment with CD19 CAR-T cells alone exhibited limited efficacy and could not even reduce tumor size. In contrast, reduction in tumor size was greater in the ibrutinib combined with CD19 CAR-T cells group than that in the CAR-T-cell alone group ($P_{\text{day}14} = 0.0618$, $P_{\text{day}21} = .0127$, $P_{\text{day}28} = .0145$) (Figure 5C). More importantly, the polytherapy group showed the best efficacy, indicating an additive effect between ibrutinib and CD19 CAR-T-cell.

In the subcutaneous tumorigenic model, the proportions of CD19 CAR-T cells in the CD19 CAR-T-cell monotherapy group and the ibrutinib combined with CD19 CAR-T cells group were analyzed. There was no difference in the proportion of CD19 CAR-T cells between the 2 groups on day 7 and day 14 ($P_{\text{day}7} = 0.1394$, $P_{\text{day}14} = 0.0812$). Afterward, the proportion of CD19 CAR-T cells began to increase and almost doubled by day 21 in the polytherapy group, a proven sign of robust CAR-T-cell activation and consequent cytotoxicity, which was absent in the monotherapy group ($P_{\text{day}21} = .0015$, $P_{\text{day}28} = 0.0207$) (Figure 5D).

3.9 | Antitumor efficacy of ibrutinib and CD19 CAR-T cells in the tail vein tumorigenic model

In the tail vein tumorigenic model, the proportion of lymphoma cells in the CD19 CAR-T-cell monotherapy group increased promptly, causing the mice to die quickly after 21 d of treatment. There was no difference in the proportion of lymphoma cells in the peripheral blood between the ibrutinib combined with CD19 CAR-T cells group and the CD19 CAR-T-cell monotherapy group ($P_{\text{day}14} = 1.0067$,

$P_{\text{day}21} = 0.6609$, $P_{\text{day}28} = 0.4502$), and there were also no differences among the ibrutinib combined with CD19 CAR-T cells group, the ibrutinib monotherapy group, and the ibrutinib combined with T cells group (Figure 6A). In addition, there was no difference in the proportion of lymphoma cells in the bone marrow between the ibrutinib combined with CD19 CAR-T cells group and the CD19 CAR-T-cell monotherapy group ($P_{\text{day}14} = 0.2091$) (Figure 6B).

In the tail vein tumorigenic model, the proportion of CD19 CAR-T cells first increased on day 7, suggesting the activation of CAR-T cells, and then declined quickly, probably due to tumor cell proliferation overwhelming the blood stream (Figure 6C).

3.10 | Western blot analysis of STAT-3 expression

Ibrutinib is a known inhibitor of constitutively active STAT-3 in CLL cells that downregulates the PD-L1 expression and further modulates an immunosuppressive microenvironment. We next tested whether a similar influence existed in Raji cells. Ibrutinib treatment was able to dephosphorylate STAT-3 promptly at 2 critical sites, Tyr705 and Ser727, indicating loss of activation (Figure 7). However, in line with other reports, PD-L1 was expressed in $0.23 \pm 0.06\%$ of Raji cells. These results suggested that beside induction of PD-L1 expression, ibrutinib might negatively regulate another inhibitory mechanism downstream of STAT-3 that would rescue the activity of CAR-T cells.

4 | DISCUSSION

Experiments in the use of CD19 CAR-T cells to treat R/R CLL are limited. A recent review described results of CD19 CAR-T-cell therapy in CLL found since the first efficacy report of this therapy in 2011.^{19,23} The efficacy CR was obtained only in 20%–30% of R/R

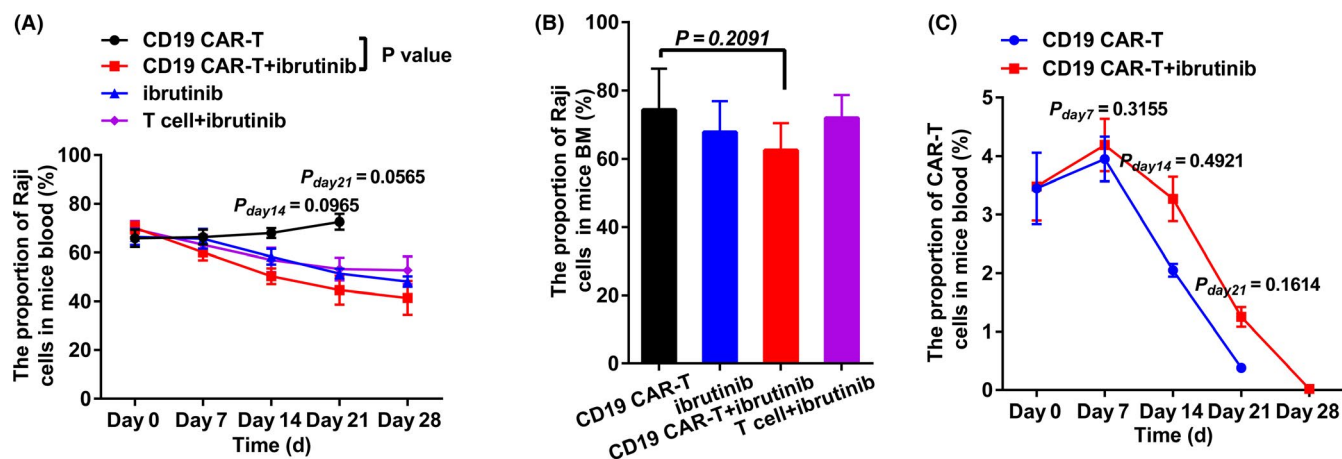


FIGURE 6 Combined effect of ibrutinib and CD19 CAR-T cells in the tail vein tumorigenic model. A, There was no difference in the proportion of lymphoma cells in the peripheral blood between the ibrutinib combined with the CD19 CAR-T-cell polytherapy group with the CD19 CAR-T-cell monotherapy group, the ibrutinib group, and the ibrutinib combined with T cells group. B, There was no difference in the proportion of lymphoma cells in the bone marrow between the ibrutinib combined with the CD19 CAR-T-cell polytherapy group and the CD19 CAR-T-cell monotherapy group. C, There was no difference in the proportion of CD19 CAR-T cells in the ibrutinib combined with CD19 CAR-T cells group and the CD19 CAR-T cells group on day 7, day 14, day 21, and day 28

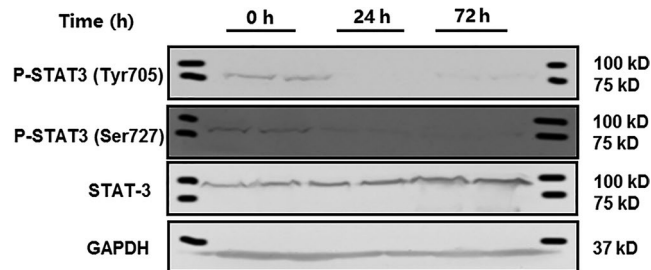


FIGURE 7 Expression of STAT-3 signaling pathway. Ibrutinib inhibited the STAT-3 in Raji cells and dephosphorylated STAT-3 at Tyr705 and Ser727 sites

CLL patients,²³ and progression-free survival was estimated at about 25% at 18 mo,^{21,22,24} which was lower for CLL than for B-ALL and DLBCL.¹⁶⁻¹⁹ The main reason might be related to T-cell dysfunction in CLL patients, resulting in decreased amplification and activity of CD19 CAR-T cells.²⁵⁻²⁷

As an oral BTK inhibitor, ibrutinib is capable of stimulating the redistribution of malignant B cells into the peripheral blood that eventually leads to obvious shrinking of enlarged lymph nodes.^{28,29} Therefore, ibrutinib therapy has produced high ORR and long-lasting remission in patients with CLL or MCL. Ibrutinib treatment in CLL patients for more than 5 mo could improve the proliferation and cytotoxic activity of T cells and their CD19 CAR-T cells.²⁶ In addition, the expression of an immunosuppressive marker, PD-1, was reduced, and might explain the function restoration of these T cells after prolonged ibrutinib treatment. Moreover, such clinical curative effects of CD19 CAR-T-cell therapy could be reproduced in patients who experienced failure of ibrutinib therapy.²¹ It will be of value to explore whether ibrutinib has homologous beneficial effect in other B-cell malignancies.

In addition to CLL, a similar synergistic effect between ibrutinib and CD19 CAR-T-cell was reported for a MCL cell line.²² However, the working concentrations of ibrutinib were 25 and 125 mg/kg/d, which is substantially above the clinically recommended dose for ibrutinib. In this study, we chose a clinically recommended dose ibrutinib (8 mg/kg/d) as we were concerned that excessive doses of ibrutinib might inhibit CAR-T cells' proliferation. We selected a patient with lack of CD19 CAR-T-cell functionality to investigate the synergistic effect of CAR-T cells with ibrutinib on a Raji cell line in vitro and in vivo. No synergistic effect was observed in vitro and in the tail vein tumorigenic mouse model. Interestingly, we confirmed the synergistic effects of ibrutinib combined with CD19 CAR-T-cell in a subcutaneous tumorigenic mice model. The reason for different results between the 2 tumorigenesis methods in mice was unclear, but it is possible that the complex tumor microenvironment in the subcutaneous tumorigenic mouse model contributed to this synergistic effect. Further studies are needed to elucidate the exact mechanism.

The mechanisms by which ibrutinib enhances T-cell function are still not sufficiently clear. Ibrutinib could enhance the function of T cells from CLL patients through BTK-dependent and BTK-independent mechanisms.²⁷ One study showed that ibrutinib

modulated the microenvironment and reduced immune suppression by downregulating the expression of programmed death-ligand-1 (PD-L1) on CLL cells.³⁰ Their further analysis showed that this effect was mediated through inhibition of the STAT3 pathway in CLL cells.³⁰ A related study found that BTK inhibitors blocked both NFATc1 and STAT-3 activation, thereby inhibiting IL-10 and PD-L1 expression.³¹ Another study showed that ibrutinib markedly increased CD4⁺ and CD8⁺ T-cell numbers and reduced PD-1 and CTLA-4 expression in CLL patients; this mechanism may involve diminished activation-induced cell death through IL-2-inducible T-cell kinase (ITK) inhibition.²⁷ Inhibition of ITK activity would lead to the inhibition of Th2 cell differentiation and promotion of Th1 cell immune response.³¹ Furthermore, in CD19 CAR-T-cell therapy, ibrutinib may promote the expansion, maintenance, and cytotoxicity of CD19 CAR-T cells in vitro.^{27,31,32} All these findings revealed that PD-L1 expression could be modulated by small molecule inhibitors to potentiate immunotherapy. In our study, the synergistic effect was greater in the ibrutinib combined with CD19 CAR-T cells group than in the ibrutinib only group in the Raji cell subcutaneous tumorigenic mouse model, rather than in the tail vein tumorigenic model. However, there was no difference in STAT-3 expression between the groups of ibrutinib with vs. without CD19 CAR-T cells. In addition, PD-L1 expression was only $0.23 \pm 0.06\%$ in Raji cells, which may indicate that non-IL-10/STAT-3/PD-L1 pathways were involved in the synergistic effect and that some other mechanism related to the microenvironment might be a possible target for ibrutinib.

In our study, we chose CD19 CAR-T cells generated from patient no. 7, who did not respond to CAR-T-cell therapy, and Raji cells, which do not express PD-L1. The Raji cell subcutaneous tumorigenic mouse model received the clinically recommended dose of ibrutinib for only 28 d. We did not observe a synergistic effect of ibrutinib and CD19 CAR-T cells on Raji cells in vitro, which is in disagreement with the results of previous studies using a MCL cell line.^{27,31,32} Nevertheless, ibrutinib could improve the curative effects of CD19 CAR-T cells in a Raji cell subcutaneous tumorigenic mice. It is plausible that our results suggested that the microenvironment might be a possible target for ibrutinib, rather than the STAT-3 signaling pathway. Further studies are required to elucidate these mechanisms and provide evidence for the use of ibrutinib in polytherapy for other types of B-cell lymphoma.

ACKNOWLEDGMENTS

We thank the patients for their participation in our experimental studies and clinical trials. We thank LetPub (www.letpub.com) for its linguistic assistance during the preparation of this manuscript.

DISCLOSURE

The authors declare no conflicts of interest for this article.

ORCID

Juan Mu  <https://orcid.org/0000-0003-2339-0892>

Qi Deng  <https://orcid.org/0000-0002-3646-4953>

REFERENCES

1. Saleh LM, Wang W, Herman SEM, et al. Ibrutinib downregulates a subset of miRNA leading to upregulation of tumor suppressors and inhibition of cell proliferation in chronic lymphocytic leukemia. *Leukemia*. 2017;31:340-349.
2. Chang BY, Francesco M, De Rooij MFM, et al. Egress of CD19(+) CD5(+) cells into peripheral blood following treatment with the Bruton tyrosine kinase inhibitor ibrutinib in mantle cell lymphoma patients. *Blood*. 2013;122:2412-2424.
3. Cheng S, Ma J, Guo A, et al. BTK inhibition targets in vivo CLL proliferation through its effects on B-cell receptor signaling activity. *Leukemia*. 2014;28:649-657.
4. Ponader S, Chen S-S, Buggy JJ, et al. The Bruton tyrosine kinase inhibitor PCI-32765 thwarts chronic lymphocytic leukemia cell survival and tissue homing in vitro and in vivo. *Blood*. 2012;119:1182-1189.
5. Mohammad DK, Nore BF, Hussain A, et al. Dual phosphorylation of Btk by Akt/protein kinase B provides docking for 14-3-3, regulates shuttling, and attenuates both tonic and induced signaling in B cells. *Mol Cell Biol*. 2013;33:3214-3226.
6. Ponader S, Burger JA. Bruton's tyrosine kinase: from X-linked agammaglobulinemia toward targeted therapy for B-cell malignancies. *J Clin Oncol*. 2014;32:1830-1839.
7. Advani RH, Buggy JJ, Sharman JP, et al. Bruton tyrosine kinase inhibitor ibrutinib (PCI-32765) has significant activity in patients with relapsed/refractory B-cell malignancies. *J Clin Oncol*. 2013;31:88-94.
8. Herman SEM, Mustafa RZ, Gyamfi JA, et al. Ibrutinib inhibits BCR and NF- κ B signaling and reduces tumor proliferation in tissue-resident cells of patients with CLL. *Blood*. 2014;123:3286-3295.
9. Byrd JC, Furman RR, Coutre SE, et al. Targeting BTK with ibrutinib in relapsed chronic lymphocytic leukemia. *N Engl J Med*. 2013;369:32-42.
10. Wang ML, Rule S, Martin P, et al. Targeting BTK with ibrutinib in relapsed or refractory mantle-cell lymphoma. *N Engl J Med*. 2013;369:507-516.
11. Rule S, Jurczak W, Jerkeman M, et al. Ibrutinib versus temsirolimus: 3-year follow-up of patients with previously treated mantle cell lymphoma from the phase 3, international, randomized, open-label RAY study. *Leukemia*. 2018;32:1799-1803.
12. Buggy JJ, Elias L. Bruton tyrosine kinase (BTK) and its role in B-cell malignancy. *Int Rev Immunol*. 2012;31:119-132.
13. Schliffke S, Akyüz N, Ford CT, et al. Clinical response to ibrutinib is accompanied by normalization of the T-cell environment in CLL-related autoimmune cytopenia. *Leukemia*. 2016;30:2232-2234.
14. Jain P, Keating M, Wierda W, et al. Outcomes of patients with chronic lymphocytic leukemia after discontinuing ibrutinib. *Blood*. 2015;125:2062-2067.
15. Maddocks KJ, Ruppert AS, Lozanski G, et al. Etiology of ibrutinib therapy discontinuation and outcomes in patients with chronic lymphocytic leukemia. *JAMA Oncol*. 2015;1:80.
16. Neelapu SS, Locke FL, Bartlett NL, et al. Axicabtagene ciloleucel CAR T-Cell therapy in refractory large B-cell lymphoma. *N Engl J Med*. 2017;377:2531-2544.
17. Schuster SJ, Bishop MR, Tam CS, et al. Tisagenlecleucel in adult relapsed or refractory diffuse large B-cell lymphoma. *N Engl J Med*. 2019;380:45-56.
18. Maude SL, Laetsch TW, Buechner J, et al. Tisagenlecleucel in children and young adults with B-cell lymphoblastic leukemia. *N Engl J Med*. 2018;378:439-448.
19. Porter DL, Levine BL, Kalos M, et al. Chimeric antigen receptor-modified T cells in chronic lymphoid leukemia. *N Engl J Med*. 2011;365:725-733.
20. Porter DL, Hwang W-T, Frey NV, et al. Chimeric antigen receptor T cells persist and induce sustained remissions in relapsed refractory chronic lymphocytic leukemia. *Sci Transl Med*. 2015;7(303):303ra139.
21. Turtle CJ, Hay KA, Hanafi L-A, et al. Durable molecular remissions in chronic lymphocytic Leukemia treated with CD19-specific chimeric antigen receptor-modified T cells after failure of ibrutinib. *J Clin Oncol*. 2017;35:3010-3020.
22. Ruella M, Kenderian SS, Shestova O, et al. The addition of the BTK inhibitor ibrutinib to anti-CD19 chimeric antigen receptor T cells (CART19) improves responses against mantle cell lymphoma. *Clin Cancer Res*. 2016;22:2684-2696.
23. Lemal R, Tournilhac O. State-of-the-art for CAR T-cell therapy for chronic lymphocytic leukemia in 2019. *J Immunother Cancer*. 2019;7:202.
24. Fraietta JA, Lacey SF, Orlando EJ, et al. Determinants of response and resistance to CD19 chimeric antigen receptor (CAR) T cell therapy of chronic lymphocytic leukemia. *Nat Med*. 2018;24:563-571.
25. Mueller KT, Maude SL, Porter DL, et al. Cellular kinetics of CTL019 in relapsed/refractory B-cell acute lymphoblastic leukemia and chronic lymphocytic leukemia. *Blood*. 2017;130:2317-2325.
26. Fraietta JA, Beckwith KA, Patel PR, et al. Ibrutinib enhances chimeric antigen receptor T-cell engraftment and efficacy in leukemia. *Blood*. 2016;127:1117-1127.
27. Long M, Beckwith K, Do P, et al. Ibrutinib treatment improves T cell number and function in CLL patients. *J Clin Invest*. 2017;127:3052-3064.
28. Burger JA, Montserrat E. Coming full circle: 70 years of chronic lymphocytic leukemia cell redistribution, from glucocorticoids to inhibitors of B-cell receptor signaling. *Blood*. 2013;121:1501-1509.
29. Burger JA, Keating MJ, Wierda WG, et al. Safety and activity of ibrutinib plus rituximab for patients with high-risk chronic lymphocytic leukaemia: a single-arm, phase 2 study. *Lancet Oncol*. 2014;15:1090-1099.
30. Kondo K, Shaim H, Thompson PA, et al. Ibrutinib modulates the immunosuppressive CLL microenvironment through STAT3-mediated suppression of regulatory B-cell function and inhibition of the PD-1/PD-L1 pathway. *Leukemia*. 2018;32:960-970.
31. Dubovsky JA, Beckwith KA, Natarajan G, et al. Ibrutinib is an irreversible molecular inhibitor of ITK driving a Th1-selective pressure in T lymphocytes. *Blood*. 2013;122:2539-2549.
32. Yin Q, Sivina M, Robins H, et al. Ibrutinib therapy increases T cell repertoire diversity in patients with chronic lymphocytic Leukemia. *J Immunol*. 2017;198:1740-1747.

How to cite this article: Liu M, Wang X, Li Z, et al. Synergistic effect of ibrutinib and CD19 CAR-T cells on Raji cells in vivo and in vitro. *Cancer Sci*. 2020;111:4051-4060. <https://doi.org/10.1111/cas.14638>